

Case Report

## Chronic otitis externa with heat shock protein 70-positive intranuclear inclusion bodies in the ceruminous gland epithelium of a Chihuahua dog

Takeru Kiuchi<sup>1</sup>, Kenichi Watanabe<sup>1\*</sup>, Shotaro Nakagun<sup>1</sup>, Kazuro Miyahara<sup>1</sup>, Noriyuki Horiuchi<sup>1</sup>, and Yoshiyasu Kobayashi<sup>1</sup>

<sup>1</sup> Department of Veterinary Medicine, Obihiro University of Agriculture and Veterinary Medicine, 2-11 Inada, Obihiro-shi, Hokkaido 080-8555, Japan

**Abstract:** A Chihuahua dog showed persistent itching in the right ear canal. Anti-inflammatory medicines and prednisolone were ineffective and total ear canal ablation was performed. Histological diagnosis was chronic otitis externa. Eosinophilic intranuclear inclusion bodies (Cowdry type A and full-type) were occasionally observed in the ceruminous gland epithelium. The inclusion bodies were negative for nucleic acid and ultrastructurally composed of fibrous structures (approximately 10 nm in width). Viral infection was initially suspected, but polymerase chain reaction tests did not detect the expected viral genes. Immunohistochemistry revealed that the inclusion bodies were positive for heat shock protein 70 (HSP70), suggesting that these bodies could be protein aggregates including HSP70. The etiology of this lesion has not been elucidated, but chronic inflammation may influence the cytoplasm-to-nuclear transportation of HSP70. To the best of our knowledge, this is the first report of canine chronic otitis externa with HSP70-positive intranuclear inclusion bodies. (DOI: 10.1293/tox.2021-0033; *J Toxicol Pathol* 2022; 35: 83–87)

**Key words:** Otitis externa, intranuclear inclusion body, heat shock protein 70, dog

Otitis externa is a common disease in dogs and cats. It may be acute or chronic and unilateral or bilateral. Major clinical signs include head shaking, odor, pain, exudate, and erythema. The causes of otitis externa are diverse and include bacterial, viral, parasitic, and fungal infections; allergic responses; immune disorders; and endocrine abnormalities<sup>1</sup>. Histological changes in otitis externa also vary with the associated causes. Generally, varying degrees of hyperplasia in the epidermis, ceruminous gland, sebaceous gland, and interstitium can be observed. Intranuclear inclusion bodies are one of the most important pathological hallmarks of viral infections. On the other hand, non-viral intranuclear inclusions may also be reported. Non-viral intranuclear inclusions are formed by nuclear membrane invagination or abnormal protein storage in the nuclei. There are no reports of otitis externa with inclusion bodies nor otitis externa associated with viral infection in domestic animals. We present a case of chronic otitis externa with heat shock protein (HSP) 70-positive intranuclear inclusion

bodies in a Chihuahua dog.

A female Chihuahua dog (aged 12 years and 8 months) was hospitalized with a chief complaint of chronic pruritus in the right ear and extremities for approximately 5 years and was treated with anti-inflammatory medications and prednisolone. The animal showed severe chronic otitis externa with calcification of the ear cartilage and proliferation of the ear canal epithelium. Total ear canal ablation was performed since the external acoustic meatus was occluded.

The ear canal was fixed in 15% neutral-buffered formalin and embedded in paraffin. Sections of 4- $\mu$ m thickness were cut and stained with hematoxylin and eosin, Masson's trichrome, periodic acid-Schiff (PAS) reaction, Feulgen reaction, and methyl green-pyronin stain. Immunohistochemistry (IHC) was performed following standard techniques using the Histofine Simple Stain MAX-PO kit (Nichirei Bioscience Inc., Tokyo, Japan) with 3,3'-diaminobenzidine (Nichirei Bioscience Inc.). The primary antibodies used for the analysis are presented in Table 1. Antigen retrieval was performed using citrate buffer (pH: 6.0). Sections were incubated with 3% H<sub>2</sub>O<sub>2</sub> for 5 min to reduce endogenous peroxidase activity. The sections were incubated with primary antibodies overnight at 4°C. After being washed with phosphate-buffered saline and Tween 20, the sections were incubated with MAX-PO polymer solution (Nichirei Bioscience Inc.) for 30 min at room temperature. The sections were lightly counterstained with Mayer's hematoxylin. To examine the involvement of pathogens in this condition,

Received: 27 May 2021, Accepted: 4 August 2021

Published online in J-STAGE: 28 August 2021

\*Corresponding author: K Watanabe (e-mail: knabe@obihiro.ac.jp)

©2022 The Japanese Society of Toxicologic Pathology

This is an open-access article distributed under the terms of the Creative Commons Attribution Non-Commercial No Derivatives

(by-nc-nd) License. (CC-BY-NC-ND 4.0: <https://creativecommons.org/licenses/by-nc-nd/4.0/>).



polymerase chain reaction (PCR) targeting intranuclear inclusion bodies of several viral forms was conducted. Total DNA was extracted from formalin-fixed paraffin-embedded (FFPE) tissue using a Nucleospin tissue kit (Macherey-Nagel GmbH & Co., Duren, Germany) following the manufacturer's instructions. The consensus primer sets and target gene fragments used for the detection of papillomavirus (MY09/11) and herpesvirus (DFA/KG1) are listed in Table 2.<sup>3</sup> The primer sets for parvovirus (NSshort F/R) and adenovirus (pVIIshort F/R) were designed using Primer-BLAST. The position of NSshort F/R was 1962-2041 in canine parvovirus (GenBank ID: M19296). The positions of pVIIshort F/R were 14010-14079 in canine adenovirus type 1 (GenBank ID: Y07760) and 14116-14185 in canine adenovirus type 2 (GenBank ID: U77082). The canine C $\mu$  gene (constant region of IgM, 133bp) was used for internal control<sup>4</sup>. DNA extracts from the FFPE tissues of natural cases (papillomavirus, bovine viral papilloma, parvovirus, canine parvoviral enteritis, adenovirus, infectious canine hepatitis, herpesvirus, and gammaherpesviral balanitis in a stranded striped dolphin) were used as positive controls for PCR. EmeraldAmp (Takara Bio Inc., Shiga, Japan) was used for DNA amplification. The thermocycling profile was as follows: initial denaturation at 98 °C for 2 min, followed by 45 cycles of denaturation at 98°C for 10 s, annealing at 55°C for 30 s, and elongation at 72°C for 30 s. All PCR products were electrophoresed on 3% agarose gel. For ultrastructural examination, formalin-fixed tissues were cut into 1-mm<sup>3</sup> specimens and postfixed in 2.5% glutaraldehyde and 1%

osmium tetroxide. After the dehydration steps, the specimens were embedded in LR white resin (Polysciences Inc., Warrington, PA, USA). Ultra-thin sections (70 nm) were cut and examined using a transmission electron microscope (H-7700, Hitachi, Tokyo, Japan).

On gross examination, the ear canal was firm and the lumen was constricted. The ear auricle showed papillary thickening and calcification. Histologically, severe diffuse hyperplasia of the epidermis was observed in the ear canal. Proliferation of the sebaceous glands, ceruminous glands, and connective tissue and moderate to severe diffuse infiltration of lymphocytes and plasma cells were observed in the dermis. The ceruminous glands were dilated and filled with foamy macrophages, neutrophils, desquamated epithelia, and cell debris (Fig. 1A). Brown pigment granules were deposited in the acinar cells and cytoplasm of macrophages. Although cellular polarity seemed to be maintained, ceruminous gland epithelia had proliferated on the luminal side. No vascular invasion, infiltrative growth over the basement membrane, nuclear atypia, or mitosis was observed. IHC revealed few positive reactions for Ki-67 (3.4%) and proliferating cell nuclear antigen (16.7%) in the acinar cells. On the other hand, some of the acinar cells exhibited a swollen nucleus with intranuclear inclusion bodies that were morphologically similar to the full-type (pale, ground-glass-like) and Cowdry type A (eosinophilic, defined with halo) inclusion bodies (Fig. 1B). The inclusions assumed an orange-to-red appearance following staining with Masson's trichrome (Fig. 1C). However, they were negative for PAS

**Table 1.** Antibodies for Immunohistochemistry

| Antibody  | Clone   | Maker                | Dilution     | Antigen retrieval                                   | Positive control  |
|-----------|---------|----------------------|--------------|---|---|
| Ki-67     | MIB-1   | DAKO                 | ready to use | Microwave 93°C 15 min 0.01M citrate buffer (pH 6.0) | proliferated cells  |
| PCNA      | PC10    | Nichirei Biosciences | ready to use | Microwave 93°C 15 min 0.01M citrate buffer (pH 6.0) | proliferated cells  |
| CK        | AE1/AE3 | DAKO                 | 1:200        | Microwave 93°C 15 min 0.01M citrate buffer (pH 6.0) | epithelial cells  |
| LC3       | PM036   | MBL                  | 1:1000       | Microwave 93°C 15 min 0.01M citrate buffer (pH 6.0) | (aggregated protein)  |
| Ubiquitin | Z0458   | DAKO                 | 1:100        | Microwave 93°C 15 min 0.01M citrate buffer (pH 6.0) | (aggregated protein)  |
| HSP70     | BRM-22  | SIGMA                | 1:4000       | Microwave 93°C 15 min 0.01M citrate buffer (pH 6.0) | ceruminous gland epithelia, sebaceous gland epithelia (cytoplasm), epidermis (granular cell and prickle cell layer) |

**Table 2.** Primer List for Viral Polymerase Chain Reaction Test

| Virus                          | Primer  | Sequence (5'-3')           |
|--------------------------------|---------|----------------------------|
| Papillomavirus                 | Forward | CGTCCMARRGGAWCTGATC        |
|                                | Reverse | GCMCAGGWCATAAAYAATGG       |
| Parvovirus                     | Forward | ACTGGGCGGAGCCTAAAATAC      |
|                                | Reverse | AGGATTGCTTGCCGCTTGTG       |
| Adenovirus                     | Forward | AGGCACTACAAGCTATTTGG       |
|                                | Reverse | GTGAGCTTGACATAAACGGG       |
| Herpesvirus                    | Forward | GAYTTYGCNAGYYTNTAYCC       |
|                                | Reverse | GTCTTGCTCACCAGNTCNACNCCYTT |
| Control gene (Canine C $\mu$ ) | Forward | TTCCCCCTCATCACCTGTGA       |
|                                | Reverse | GGTTGTTGATTGCACTGAGG       |



reaction, Feulgen reaction, and methyl green-pyronin stain. IHC revealed that the inclusions were positive for HSP70, whereas the ceruminous gland epithelia (with or without inclusion bodies), sebaceous gland epithelia, granular cell layer, and prickle cell layer of the epidermis were also weakly positive for HSP70 (Fig. 1D). The inclusions were negative for other antibodies (CK, LC3, and ubiquitin). PCR assays targeting adenovirus, parvovirus, herpesvirus, and papillomavirus were performed, but no positive amplifications were detected. Electron microscopy revealed that Cowdry type A inclusion bodies consisted of non-branching fibrillar components approximately 10 nm in width (Fig. 2A). In the swollen nucleus with full-type inclusion bodies, the nucleoplasm was scattered and fibrillar components, cytoplasmic matrix, and virus particles were not observed (Fig. 2B).

Intranuclear inclusion bodies are categorized as viral

or non-viral. Viral intranuclear inclusions are formed following infection by foreign viruses. Non-viral intranuclear inclusions are formed by nuclear membrane invagination or abnormal protein storage. The prominent viruses that form intranuclear inclusion bodies in dogs include papillomavirus, herpesvirus, parvovirus, adenovirus, and polyomavirus. Initially, we suspected that these viruses were involved in the lesion from the present case. We investigated the possibility of infection with papillomavirus, herpesvirus, parvovirus, and adenovirus. However, the inclusion bodies were negative for Feulgen reaction and PCR. Moreover, no viral particles were observed under electron microscope. Subsequently, we investigated the possibility of RNA virus infection, but the inclusion bodies were negative for methyl green-pyronin staining. These results suggested that the formation of intranuclear inclusions was not due to viral infec-

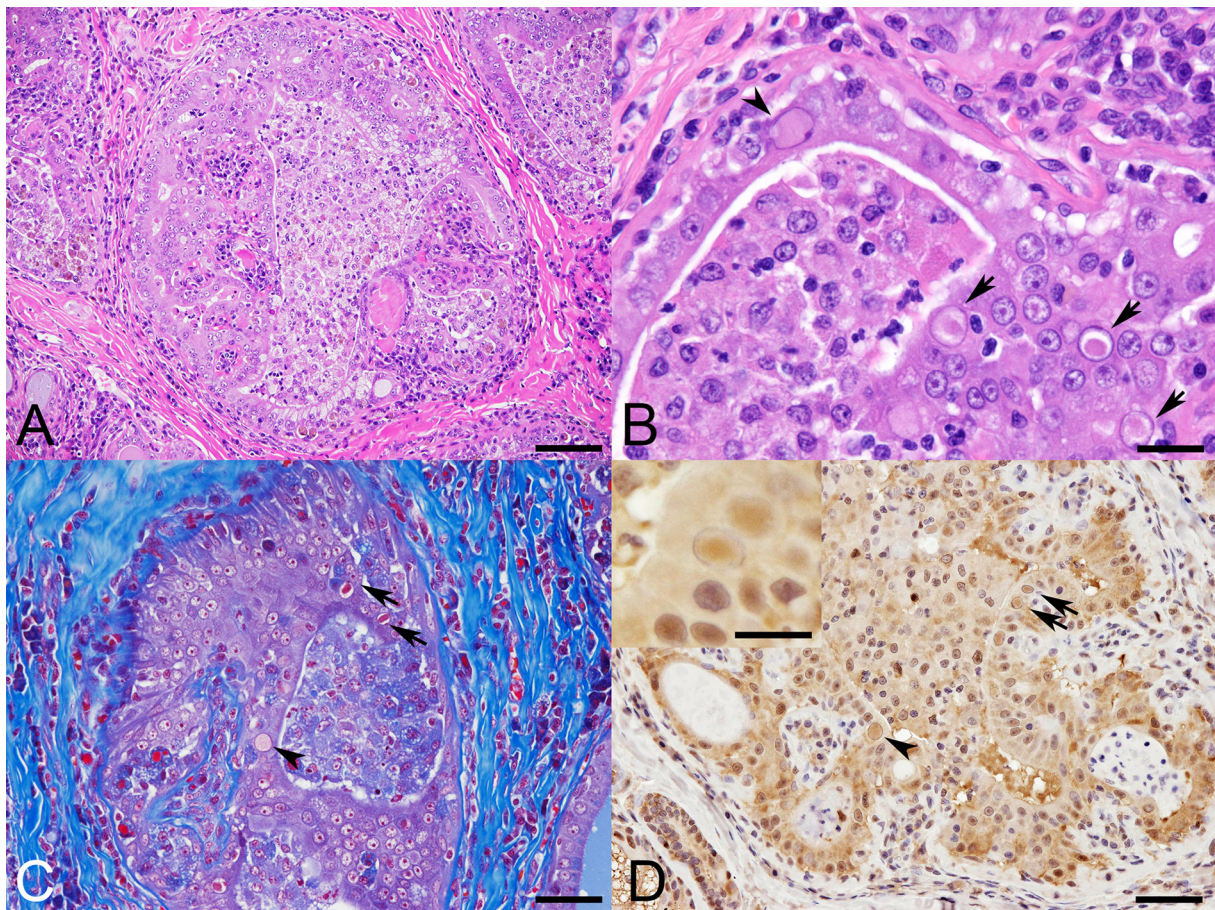


**Fig. 1.** Histopathological features of the case.

- (A) The ceruminous gland is ectatic and shows accumulation of foamy macrophages, neutrophils, shedding epithelia, and debris (hematoxylin-eosin [HE] stain, bar=100  $\mu$ m).
- (B) High magnification of (A) shows intranuclear inclusion bodies. Full-type inclusions with ground-glass appearance (arrowhead) and Cowdry type A inclusions (arrow) with halos can be observed in the ceruminous gland epithelia (HE stain, bar=25  $\mu$ m).
- (C) Masson's trichrome staining of the seruminous gland shows full-type inclusions in orange (arrowheads) and Cowdry type A inclusions in red (arrows) (Masson's trichrome stain, bar=50  $\mu$ m).
- (D) Immunohistochemistry of the ceruminous gland shows that full-type inclusions (arrowhead) and Cowdry type A inclusions (arrow) are immunopositive for heat shock protein 70 (HSP70) (immunohistochemistry for HSP70, bar=50  $\mu$ m). Inset indicates Cowdry type A inclusions (bar=20  $\mu$ m).



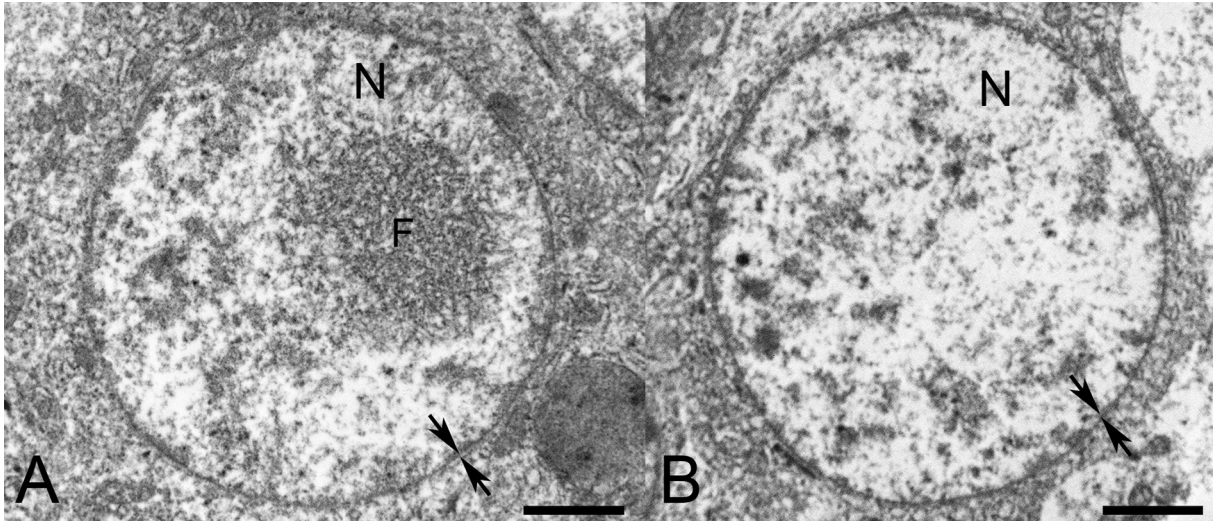


**Fig. 2.** Ultrastructure of the inclusion bodies.

(A) The Cowdry type A inclusion bodies exhibit non-branched fibrillar components approximately 10 nm in width (bar=2.0  $\mu$ m). No membranous structure is observed around the fibrillar structure. There is no viral particle in the nucleus.

(B) The swollen nucleus contains full-type inclusion bodies. The nucleoplasm is scattered and neither viral particle nor fibrillar components are observed (bar=2.5  $\mu$ m).

Arrow: nuclear membrane, N: nuclei; F: fibrillar components.

tions in the present case.

Non-viral intranuclear inclusions formed by nuclear membrane invagination have been reported in tumors such as papillary thyroid carcinoma<sup>5-8</sup>, mammary gland tumors, and ductal adenoma<sup>5</sup>. The inclusion bodies in these cases were defined as nuclear membranes. Nuclear invagination is a type of nuclear atypia. Therefore, neoplastic cells sometimes have wrinkles and notches in the nucleus. In the present case, there was no membranous structure at the border between the inclusion bodies and the nucleoplasm. Additionally, the acinar cells did not exhibit any wrinkles or notches in the nuclear membrane. The inclusion bodies were negative for cytokeratin and showed dyeability different from that of cytoplasm for special stains. No intracellular organelles were observed on ultrastructural examination. Based on these results, we ruled out the possibility of nuclear membrane invagination.

Non-viral inclusions are also formed by protein shuttling from the cytosol to the nucleus. Some studies have reported intranuclear storage of surfactant proteins in pulmonary adenocarcinomas<sup>5, 9, 10</sup>, immunoglobulin in lymphomas<sup>5</sup>, and glycogen in degenerated hepatocytes<sup>4</sup>. In addition, an *in vitro* study showed that an intranuclear filamentous body was formed with HSP70 that translocated to the nucleus under heat-shock treatment in cultured rat fibroblasts<sup>11</sup>. Under stress conditions, multigene stress protein families are upregulated and synthesized to avoid cellular damage from various stressful stimuli such as heat stress, inflammation, and oxidative stress<sup>9</sup>. The HSP family is a major group of stress proteins with molecular weights ranging from 28 to 110 kDa. The HSP family has the ability to protect cells by binding to abnormal and degenerated proteins<sup>9</sup>. HSP70

is a chaperone molecule that acts as a central hub in proteostasis, thereby assisting in protein folding. In humans, HSP70 has 13 isoforms. Among these, three are expressed in the cytosol/nucleus (HSPA1A, HSPA1B, and HSPA6), one is expressed in the endoplasmic reticulum (HSPA5), and two are expressed in undetermined location (HSPA12A and HSPA12B). These six isoforms are inducible under stress conditions<sup>11</sup>. In humans, HSPA1 is weakly expressed in the epidermis under physiological conditions, but its level can be elevated in pathological conditions (well-examined in tumor cases)<sup>12</sup>. It has also been reported that HSP70 is upregulated in canine cutaneous tumors and tumor-like regions<sup>13</sup>. In the present case, severe inflammation was observed in the ceruminous glands. Moreover, the cytoplasm and/or nucleus of the ceruminous gland epithelial cells were weakly positive for HSP70 with or without inclusion bodies. These findings suggested that the inclusion bodies in the present case were formed by upregulation and protein shuttling of HSP70 from the cytosol to the nucleus under persistent inflammatory stress. There are very few reports on intranuclear inclusions with HSP. We reported an atypical case of chronic otitis externa with non-viral intranuclear inclusion bodies.

**Disclosure of Potential Conflicts of Interest:** The authors declare that there are no conflicts of interest associated with this manuscript.

**Acknowledgments:** The authors would like to thank Akiko Tomikawa for her technical support. This work was supported by JSPS KAKENHI (Grant Number 19K15994).

## References

1. Carlotti DN. Diagnosis and medical treatment of otitis externa in dogs and cats. *J Small Anim Pract.* **32**: 394–400. 1991. [[CrossRef](#)]
2. Lurchachaiwong W, Junyangdikul P, Payungporn S, Chansaenroj J, Sampatanukul P, Tresukosol D, Termrungruanglert W, and Poovorawan Y. Relationship between hybrid capture II ratios and DNA amplification of E1, E6 and L1 genes used for the detection of human papillomavirus in samples with different cytological findings. *Asian Pac J Allergy Immunol.* **27**: 217–224. 2009. [[Medline](#)]
3. VanDevanter DR, Warrener P, Bennett L, Schultz ER, Coulter S, Garber RL, and Rose TM. Detection and analysis of diverse herpesviral species by consensus primer PCR. *J Clin Microbiol.* **34**: 1666–1671. 1996. [[Medline](#)] [[CrossRef](#)]
4. Burnett RC, Vernau W, Modiano JF, Olver CS, Moore PF, and Avery AC. Diagnosis of canine lymphoid neoplasia using clonal rearrangements of antigen receptor genes. *Vet Pathol.* **40**: 32–41. 2003. [[Medline](#)] [[CrossRef](#)]
5. Ip YT, Dias Filho MA, and Chan JKC. Nuclear inclusions and pseudoinclusions: friends or foes of the surgical pathologist? *Int J Surg Pathol.* **18**: 465–481. 2010. [[Medline](#)] [[CrossRef](#)]
6. Cracolici V, Krausz T, and Cipriani NA. Ubiquitin immunostaining in thyroid neoplasms marks true intranuclear cytoplasmic pseudoinclusions and may help differentiate papillary carcinoma from NIFTP. *Head Neck Pathol.* **12**: 522–528. 2018. [[Medline](#)] [[CrossRef](#)]
7. Glant MD, Berger EK, and Davey DD. Intranuclear cytoplasmic inclusions in aspirates of follicular neoplasms of the thyroid. A report of two cases. *Acta Cytol.* **28**: 576–580. 1984. [[Medline](#)]
8. Zhu YZ, Li WP, Wang ZY, Yang HF, He QL, Zhu HG, and Zheng GJ. Primary pulmonary adenocarcinoma mimicking papillary thyroid carcinoma. *J Cardiothorac Surg.* **8**: 131–134. 2013. [[Medline](#)] [[CrossRef](#)]
9. Benjamin IJ, and McMillan DR. Stress (heat shock) proteins: molecular chaperones in cardiovascular biology and disease. *Circ Res.* **83**: 117–132. 1998. [[Medline](#)] [[CrossRef](#)]
10. Noeman EC. Interpretation of acute cell injury. In: *Ultrastructural Pathology an Introduction to Interpretation.* EC Noeman (ed). Iowa State University Press, Ames. 75–101. 1994.
11. Welch WJ, and Suhan JP. Morphological study of the mammalian stress response: characterization of changes in cytoplasmic organelles, cytoskeleton, and nucleoli, and appearance of intranuclear actin filaments in rat fibroblasts after heat-shock treatment. *J Cell Biol.* **101**: 1198–1211. 1985. [[Medline](#)] [[CrossRef](#)]
12. Scieglinska D, Krawczyk Z, Sojka DR, and Gogler-Piğłowska A. Heat shock proteins in the physiology and pathophysiology of epidermal keratinocytes. *Cell Stress Chaperones.* **24**: 1027–1044. 2019. [[Medline](#)] [[CrossRef](#)]
13. Monari M, Foschi J, Forteguerra EB, Valgimigli S, Zanatta M, Capitani O, and Serrazanetti GP. Evaluation of HSP70, 27 and TNF-alpha expression [corrected] in different canine cutaneous and gland diseases. *Vet Res Commun.* **33**(Suppl 1): 109–111. 2009. [[Medline](#)] [[CrossRef](#)]